

See discussions, stats, and author profiles for this publication at: <https://www.researchgate.net/publication/259251222>

# Reaction of NO<sub>2</sub> with Selected Conjugated Alkenes

ARTICLE *in* THE JOURNAL OF PHYSICAL CHEMISTRY A · DECEMBER 2013

Impact Factor: 2.69 · DOI: 10.1021/jp408771r · Source: PubMed

---

READS

48

7 AUTHORS, INCLUDING:



**François Bernard**

National Oceanic and Atmospheric Administra...

16 PUBLICATIONS 94 CITATIONS

SEE PROFILE



**Xinming Wang**

Chinese Academy of Sciences

176 PUBLICATIONS 3,687 CITATIONS

SEE PROFILE



**Jian-Min Chen**

Fudan University

166 PUBLICATIONS 2,678 CITATIONS

SEE PROFILE

# Reaction of NO<sub>2</sub> with Selected Conjugated Alkenes

François Bernard,<sup>†</sup> Mathieu Cazaunau,<sup>†</sup> Yujing Mu,<sup>‡</sup> Xinming Wang,<sup>§</sup> Véronique Daële,<sup>†</sup> Jianmin Chen,<sup>||</sup> and Abdelwahid Mellouki<sup>\*,†,||</sup>

<sup>†</sup>Institut de Combustion, Aérodynamique, Réactivité et Environnement (ICARE), CNRS (UPR 3021)/OSUC, 1C Avenue de la Recherche Scientifique, 45071 Orléans Cedex 2, France

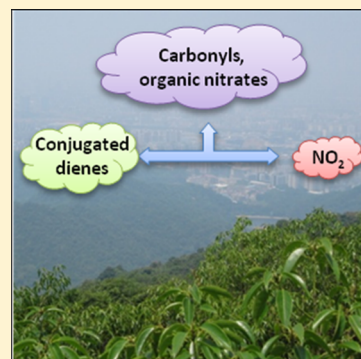
<sup>‡</sup>Research Center for Eco-environmental of Sciences, Chinese Academy of Sciences, Beijing 100085, China

<sup>§</sup>State Key Laboratory of Organic Geochemistry, Guangzhou Institute of Geochemistry, Chinese Academy of Sciences, Guangzhou 510640, China

<sup>||</sup>Environment Research Institute/School of Environmental Science & Engineering, Shandong University, Shandong 250100, China

## S Supporting Information

**ABSTRACT:** The gas phase reactions of selected alkenes (isoprene, myrcene, ocimene, and 1,3-cyclohexadiene) with NO<sub>2</sub> under dark condition have been investigated at  $T \sim 298$  K and  $P \sim 760$  Torr of purified air. The kinetic studies were performed under pseudo-first-order conditions using a large excess of NO<sub>2</sub> concentration to those of the alkenes. The rate coefficients (in  $10^{-19}$  cm<sup>3</sup> molecule<sup>-1</sup> s<sup>-1</sup>) obtained are  $1.1 \pm 0.2$  for isoprene,  $2.5 \pm 0.3$  for myrcene,  $8.5 \pm 1.2$  for ocimene, and  $15 \pm 1$  for 1,3-cyclohexadiene. Several products were identified by using in situ Fourier transform infrared (FT-IR) spectrometry, and acetone was found to be the major product from the reactions of NO<sub>2</sub> with myrcene and ocimene, with a formation yield of  $22 \pm 3\%$  and  $26 \pm 7\%$ , respectively. The oxidation products from the reactions of NO<sub>2</sub> with isoprene and 1,3-cyclohexadiene were found to be mainly nitro compounds identified by FT-IR spectroscopy. Reaction mechanisms were proposed to account for the products observed.



## 1. INTRODUCTION

In the atmosphere, alkenes are known to react with the main gas phase oxidants (OH and nitrate radicals, ozone, and chlorine atoms).<sup>1,2</sup> It is commonly assumed that the reaction with NO<sub>2</sub> is a negligible atmospheric removal process for these species because the reaction rate coefficients of NO<sub>2</sub> with alkenes are slow under atmospheric conditions ( $<10^{-20}$  cm<sup>3</sup> molecule<sup>-1</sup> s<sup>-1</sup>).<sup>3–6</sup> However, this process could be important with dienes and polyconjugated alkenes during the smog chamber experiments where very often high concentrations of reactants are used. Indeed, some of the previous studies on the reactions of NO<sub>2</sub> with dienes and polyconjugated alkenes indicate that these reactions could contribute to their consumption under high NO<sub>x</sub> conditions.<sup>4,5</sup>

In this work, we report a kinetic and mechanistic study of the reaction of NO<sub>2</sub> with isoprene, 1,3-cyclohexadiene, myrcene, and ocimene. These VOCs have been chosen according to their emission rates into the atmosphere,<sup>7</sup> and their reactivities toward NO<sub>2</sub> under dark conditions.<sup>8,9</sup> The reactions rate coefficients were determined and the oxidation products tentatively assigned and quantified using FT-IR spectroscopy. So far, the reactions of NO<sub>2</sub> with ocimene and myrcene have been investigated only as interfering reactions but not as central systems.<sup>10,11</sup> Acetone has been identified as a product from both reactions in the dark.<sup>10,11</sup> However, the NO<sub>2</sub>-initiated degradation mechanism of these two compounds is still not defined. Each of the NO<sub>2</sub>-initiated oxidation of isoprene and 1,3-cyclohexadiene has been subject to only one study.<sup>3,8</sup>

## 2. EXPERIMENTAL METHODS

The experiments have been carried out using the 7300 L ICARE Teflon chamber<sup>12,13</sup> in  $P \approx 1013$  mbar of purified air at  $T = 298 \pm 2$  K with a relative humidity of  $\sim 5\%$ . Reactants that are liquids under ambient conditions were introduced into the chamber by injecting aliquot amounts of liquid in a stream of purified air. Gaseous reactants were injected into the chamber using a calibrated gas cylinder equipped with pressure sensors. Two fans installed into the chamber ensured rapid mixing of reactants in few minutes. The concentrations of NO<sub>x</sub> (NO and NO<sub>2</sub>) were continuously monitored by a NO<sub>x</sub>–NO–NO<sub>2</sub> analyzer using chemiluminescence method (Thermo Environment 42i or/and Horiba APNA-360). SF<sub>6</sub> was added to the gas mixture to assess the dilution rate due to added flow in the chamber compensating sampling flows by the monitors.

Organic reactants and products were monitored by an in situ Fourier transform infrared spectrometer (Nicolet 5700 Magna) coupled to a white-type mirror system, resulting in a 129–148 m optical path length. Infrared spectra were recorded every 2–10 min by coadding 40–300 interferograms with a resolution of 1 cm<sup>-1</sup>. A gas chromatograph coupled to photoionization detector (GC-PID, DXDZ GC-4400) was also used for the measurements of the reactants and gas phase products. The

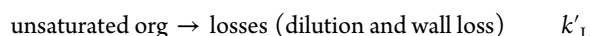
Received: September 2, 2013

Revised: December 7, 2013

Published: December 9, 2013

GC-PID is equipped with a VUV lamp with transparent light as low as 110 nm. The organic compounds were separated on a chromatographic column of 10% SE 30, PAW-HMPS (capillary column, 20 m length and 0.5 mm i.d.). An acquisition time of GC-PID was fixed at 30 min. Synthetic air (>99.999%) was used as the carrier gas with a flow rate of 10–20 mL min<sup>-1</sup>. A six-port valve equipped with an injection loop of 1 mL connected to the GC, and the loop was flushed by the reaction gas mixture at 350 mL min<sup>-1</sup> for 1 min before injection. The temperature of the column was controlled from 40 to 60 °C according to the studied chemical systems.

**2.1. Kinetic Measurements.** Most of the kinetic experiments were carried out under pseudo-first-order conditions with  $[\text{NO}_2]_0 \gg [\text{unsaturated organics}]_0$ . Under these conditions, the unsaturated organics are subject to the following removal processes:



where  $k$  is the bimolecular rate coefficient of the  $\text{NO}_2$  reaction with the unsaturated organic and  $k'_L$  is the loss rate of the unsaturated organic due to both dilution and wall losses. Under these conditions, the unsaturated organics concentration–time profiles followed the pseudo-first-order rate law:

$$[\text{unsaturated org}] = [\text{unsaturated org}]_0 \times \exp(-(k'_L + k') \times t) \quad (1)$$

with  $k' = k[\text{NO}_2]_0$ . ( $k' + k'_L$ ) is derived from the slope of the plot of  $\ln([\text{unsaturated org}]_0/[\text{unsaturated org}]_t)$  versus reaction time.  $k'_L$  is obtained by following the decay rate of the unsaturated organics in the absence of  $\text{NO}_2$ . Plots of ( $k' + k'_L$ ) versus the concentration of the unsaturated organics for the reaction of  $\text{NO}_2$  were linear and the absolute rate coefficients,  $k$ , were derived from the least-squares fit of the straight lines. The quoted error originates from two-standard deviation from the slope ( $2\sigma$ ).

The rate coefficients of both isomers of ocimene (*cis* and *trans*) were also measured using the relative rate method in which the relative disappearance rate of these species and that of myrcene used as reference compound were monitored in parallel in the presence of  $\text{NO}_2$ . The reaction rate coefficients can then be derived from the equation:

$$\ln\left(\frac{[\text{ocimene}]_{t_0}}{[\text{ocimene}]_t}\right) - k_L(\text{ocimene}) \times t = \frac{k_{\text{ocimene}}}{k_{\text{myrcene}}} \left( \ln\left(\frac{[\text{myrcene}]_{t_0}}{[\text{myrcene}]_t}\right) - k_L(\text{myrcene}) \times t \right)$$

where  $[\text{ocimene}]_{t_0}$ ,  $[\text{ocimene}]_t$ ,  $[\text{myrcene}]_{t_0}$  and  $[\text{myrcene}]_t$  represent the concentrations of ocimene (*cis*- or *trans*-ocimene) and myrcene at reaction time  $t_0$ ,  $[\text{ocimene}]_t$  and  $[\text{myrcene}]_t$  are the corresponding concentrations at time  $t$ ,  $k_{\text{ocimene}}$  and  $k_{\text{myrcene}}$  are the rate constants of the reaction of  $\text{NO}_2$  with *cis*- or *trans*-ocimene and myrcene, respectively. To account for dilution and wall processes, the pseudo-first-order decay rates of *cis*- and *trans*-ocimene and myrcene,  $k_L(\text{ocimene})$  and  $k_L(\text{myrcene})$ , respectively, have been estimated in the absence of  $\text{NO}_2$ . Plots of  $\ln([\text{ocimene}]_{t_0}/[\text{ocimene}]_t) - k_L(\text{ocimene}) \times t$  versus  $\ln([\text{myrcene}]_{t_0}/[\text{myrcene}]_t) - k_L(\text{myrcene}) \times t$  should be

linear and pass through the origin and have a slope  $k_{\text{ocimene}}/k_{\text{myrcene}}$ . The quoted uncertainties on the obtained rate coefficients originate from the uncertainties of the reference rate coefficient associated to the value of the slope (two standard deviation,  $2\sigma$ ).

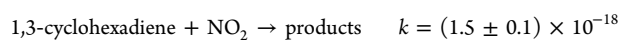
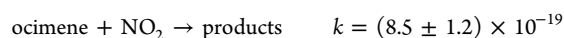
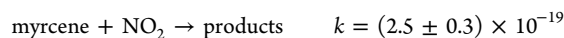
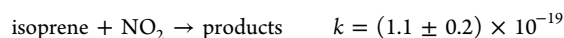
**2.2. Product Identification.** Experiments were performed in conditions similar to those of the kinetic studies (pseudo-first-order conditions). Time–concentration profiles of identified products have been corrected from dilution losses using the dilution rate constant of  $\text{SF}_6$ . When  $\text{SF}_6$  was not added to the mixture, a value of  $1.1 \times 10^{-5} \text{ s}^{-1}$  was used. Experimental time duration was extended to 4 h. Quantitative measurement of oxidation products using FT-IR spectroscopy was based on calibrated IR spectra when available. Time–concentration profiles of nitro compounds have not been corrected for the loss due to further reaction and loss to the wall. The molar product yields were derived from the average of each individual experiment and the resulted error corresponds to one-standard deviation ( $1\sigma$ ) on this average.

### 3. CHEMICALS

The purity and the origin of the chemicals used in this work are isoprene (99%, Sigma-Aldrich), 1,3-cyclohexadiene (98%, Alfa Aesar), myrcene (90%, Sigma-Aldrich), ocimene ( $\geq 90\%$ , composed of  $\geq 25\%$  of the *cis*-ocimene and  $\geq 58\%$  for the *trans*-ocimene, International Flavors and Fragrances), di-*n*-butyl ether ( $\geq 99\%$ , Sigma Aldrich), and  $\text{NO}_2$  (1% in  $\text{N}_2$ , Air liquide). The sample of ocimene contains about 68% for the *trans*-ocimene and 32% for the *cis*-ocimene.

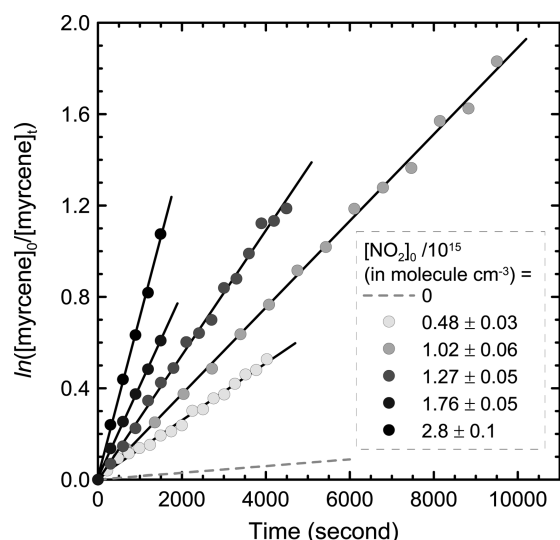
### 4. RESULTS AND DISCUSSION

**4.1. Kinetic Measurements.** The loss rates of the organic compounds in absence of  $\text{NO}_2$  were on the order of  $k_L = (1.1–1.6) \times 10^{-5} \text{ s}^{-1}$ . To achieve the pseudo-first-order conditions, the initial concentrations (in molecules  $\text{cm}^{-3}$ ) were  $[\text{alkenes}]_0 = (1.8–16.3) \times 10^{13}$ ;  $[\text{NO}_2]_0 = (0.31–3.0) \times 10^{15}$ . Unsaturated organics were monitored using FT-IR spectroscopy over the following wavenumbers (in  $\text{cm}^{-1}$ ): isoprene, 900; myrcene, 900; ocimene, 900 and 989; 1,3-cyclohexadiene, 3055 and 2837. Experimental durations were from 10 to 110 min. Typical plots of  $\ln([\text{alkenes}]_0/[\text{alkenes}]_t)$  versus time under different concentrations of  $\text{NO}_2$  are displayed in Figure 1. The rate coefficients,  $k$ , are derived from the slopes of the linear fits originated from the plots of  $k'$  versus  $\text{NO}_2$  concentrations (Figure 2). Experimental conditions for each run and the corresponding results can be found in the Supporting Information. The rate coefficient values derived (in  $\text{cm}^3 \text{ molecule}^{-1} \text{ s}^{-1}$ ) at  $T = 299 \pm 3 \text{ K}$  and  $P = 760 \text{ Torr}$  are



The quoted errors represent two-standard deviation ( $2\sigma$ ) from the least-squares analysis.

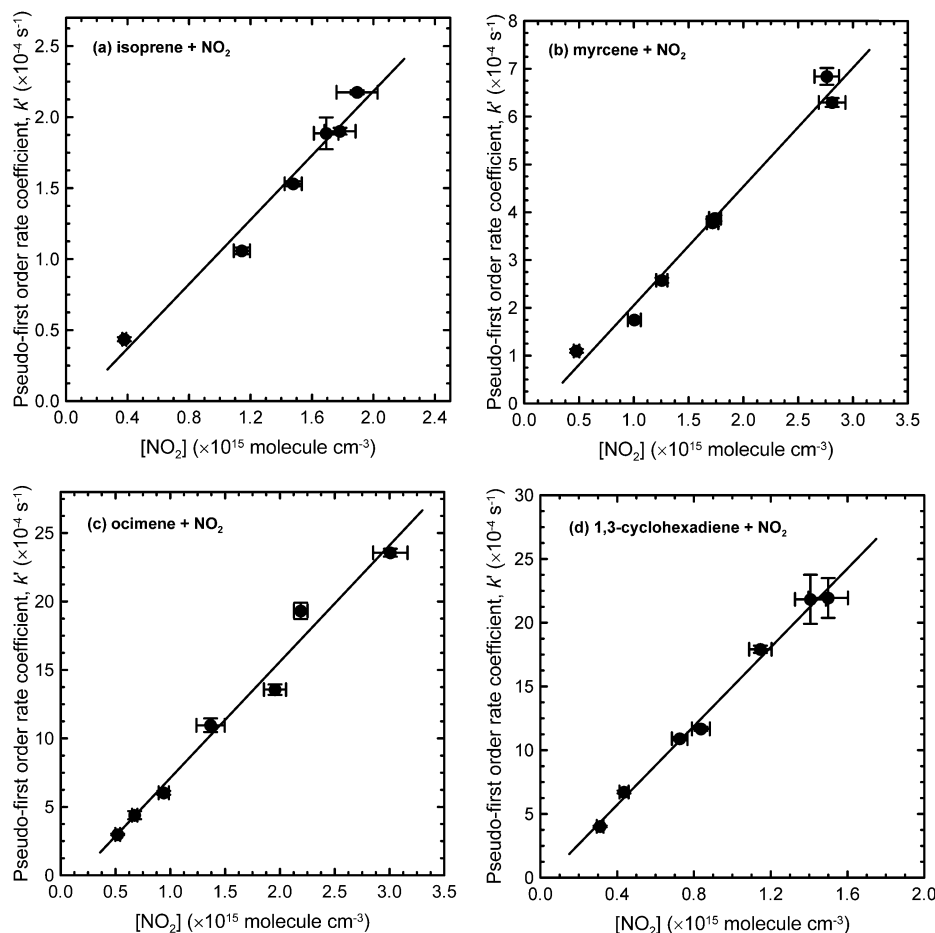
In the gas phase,  $\text{NO}_2$  coexists with its dimer  $\text{N}_2\text{O}_4$  according to the equilibrium reaction  $2\text{NO}_2 \leftrightarrow \text{N}_2\text{O}_4$ . Using the equilibrium constant,  $K = 2.5 \times 10^{-19} \text{ cm}^3 \text{ molecule}^{-1} \text{ s}^{-1}$ , for this equilibrium, it is estimated that  $\text{N}_2\text{O}_4$  in our system under the highest  $\text{NO}_2$  concentrations used in this work (up to



**Figure 1.** Pseudo-first-order experiments from the  $\text{NO}_2$ -initiated reaction of myrcene.

$3 \times 10^{15} \text{ cm}^3 \text{ molecule}^{-1}$ ) was less than 0.08% of the  $\text{NO}_2$  levels. At these concentrations and assuming the same reactivity, the dimer would not impact the chemistry occurring in our experimental system. The absolute method did not enable us to make a difference between the reactivity of the ocimene isomers (*cis* and *trans*) as the samples used in our

study contained both isomers and from the IR analysis we could not distinguish between these two species. Hence, we performed further measurements using the relative rate method and GC-PID as analytical tool. However, a significant overlap of both chromatographic peaks was observed. Therefore, the quantification has been performed using the peak height. Assuming the same response factors for both isomers, the ratios *cis*- and *trans*-ocimene in the reagent were found to be 28% and 72%, respectively, which was in agreement with the composition stated by the supplier. The initial concentrations of ocimene, myrcene, and  $\text{NO}_2$  used were (in  $10^{13} \text{ molecules cm}^{-3}$ ) 4.9, 6.2, and 6.4, respectively. The initial concentration of NO (as impurity) in the gas mixture was about  $2.5 \times 10^{11} \text{ molecules cm}^{-3}$ . The presence of NO may lead to the possible formation of OH radicals through the reaction  $\text{NO} + \text{HO}_2 \rightarrow \text{OH} + \text{NO}_2$ , which could contribute to an additional consumption of the organic reactants, resulting in an extra uncertainty on the measured rate coefficients. Therefore, di-*n*-butyl ether was added in excess ( $3.8 \times 10^{14} \text{ molecules cm}^{-3}$ ) to the gas mixture to suppress OH radicals formation ( $k(\text{di-}n\text{-butyl ether} + \text{OH}) = 2.8 \times 10^{-11} \text{ cm}^3 \text{ molecule}^{-1} \text{ s}^{-1}$ ).<sup>14</sup> The plot of  $(\ln([\text{ocimene}]_0/[\text{ocimene}]_t) - k_L(\text{ocimene})_t)$  versus  $(\ln([\text{myrcene}]_0/[\text{myrcene}]_t) - k_L(\text{myrcene})_t)$  is shown in the Supporting Information.  $k_L(\text{cis/trans-ocimene})$  and  $k_L(\text{myrcene})$  represent the first-order decay rates of *cis/trans*-ocimene and myrcene in the absence of  $\text{NO}_2$ , which were estimated to be  $\sim 1.4 \times 10^{-5} \text{ s}^{-1}$ . Under these experimental conditions, the reaction of ocimene and myrcene with  $\text{NO}_2$



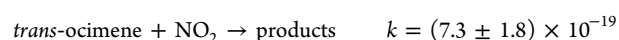
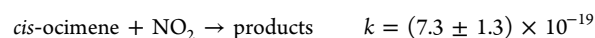
**Figure 2.** Plot of absolute rate data for the  $\text{NO}_2$  reactions with isoprene (a), myrcene (b), ocimene (c), and 1,3-cyclohexadiene (d).

Table 1. Summary of the Rate Coefficients of Studied Alkenes by Dark Reaction with NO<sub>2</sub> in the Gas Phase and Compared to the Literature<sup>a</sup>

alkenes	T (K)	no. of runs	k (cm <sup>3</sup> molecule <sup>-1</sup> s <sup>-1</sup> )	ref
isoprene	298 ± 2	6	(1.1 ± 0.2) × 10 <sup>-19</sup>	this work, <i>b</i>
	NI	5	(1.15 ± 0.08) × 10 <sup>-19</sup>	3, <i>b</i>
	NI	1	(1.8 ± 0.3) × 10 <sup>-19</sup>	15, <i>c</i>
	AT	7	(1.8 ± 0.3) × 10 <sup>-19</sup>	4, <i>c</i>
	295 ± 2	NI	(1.63 ± 0.13) × 10 <sup>-19</sup>	16, <i>d</i>
	295 ± 2	NI	(1.03 ± 0.03) × 10 <sup>-19</sup>	5, <i>b</i>
	296	8	(1.14 ± 0.07) × 10 <sup>-19</sup>	6, <i>d</i>
	298 ± 1	7	(2.5 ± 0.3) × 10 <sup>-19</sup>	this work, <i>b</i>
myrcene	NI	NI	(2.9 ± 0.3) × 10 <sup>-19</sup>	10
	297 ± 2	NI	2.9 × 10 <sup>-19</sup>	11
	294 ± 2	1	(2.6 ± 0.2) × 10 <sup>-19</sup>	17, <i>b</i>
	299 ± 2	7	(8.5 ± 1.2) × 10 <sup>-19</sup>	this work, <i>b</i>
ocimene	297 ± 2	1	1.0 × 10 <sup>-18</sup>	11
	294 ± 2	NI	(8.9 ± 0.4) × 10 <sup>-19</sup>	17, <i>d, f</i>
	297 ± 1	1	(7.3 ± 1.3) × 10 <sup>-19</sup>	this work, <i>e</i>
<i>cis</i> -ocimene	297 ± 1	1	(7.3 ± 1.8) × 10 <sup>-19</sup>	this work, <i>e</i>
<i>trans</i> -ocimene	298 ± 1	7	(1.5 ± 0.1) × 10 <sup>-18</sup>	this work, <i>b</i>
1,3-cyclohexadiene	296	5	(1.75 ± 0.15) × 10 <sup>-18</sup>	8, <i>b</i>
			(1.7 ± 0.2) × 10 <sup>-18</sup>	4, <i>e</i>
			(1.9 ± 0.3) × 10 <sup>-18</sup>	4, <i>c</i>
			(1.78 ± 0.22) × 10 <sup>-18</sup>	5, <i>b</i>

<sup>a</sup>AT: ambient temperature. NI: not indicated. <sup>b</sup>Pseudo-first-order conditions (loss rate of the alkene). <sup>c</sup>Second-order conditions (loss rates of both reactants). <sup>d</sup>Pseudo-first-order conditions (loss rate of NO<sub>2</sub>). <sup>e</sup>Relative rate conditions. <sup>f</sup>Rate coefficients of isomers *cis* and *trans* identical within ~7%.

accounted, respectively, for 84% and 63% of their total decay. The values of the rate coefficient ratios obtained are  $k(\text{trans-ocimene} + \text{NO}_2)/k(\text{myrcene} + \text{NO}_2) = 2.9 \pm 0.2$  and  $k(\text{trans-ocimene} + \text{NO}_2)/k(\text{myrcene} + \text{NO}_2) = 2.9 \pm 0.4$ . These results were placed on the absolute basis by multiplying the ratios by  $k(\text{myrcene} + \text{NO}_2) = (2.5 \pm 0.3) \times 10^{-19} \text{ cm}^3 \text{ molecule}^{-1} \text{ s}^{-1}$ . The rate coefficients derived for the reactions of NO<sub>2</sub> with ocimene isomers are (in cm<sup>3</sup> molecule<sup>-1</sup> s<sup>-1</sup>):



Errors on the rate coefficients originated from the slopes of the linear fit adding the error to the rate coefficient of the reference compound. Absolute error on the rate coefficient is equivalent to two standard deviations (2σ).

The rate coefficients compared to the literature data are summarized in Table 1. For isoprene, the reported values are in the range  $(1.0\text{--}1.8) \times 10^{-19} \text{ molecules cm}^{-3} \text{ s}^{-1}$  at  $297 \pm 2 \text{ K}$  and  $P \sim 760 \text{ Torr}$  and could be considered in fair agreement regarding the low reactivity and the difficulties to extract a precise rate coefficient value for this reaction under these conditions.

The rate coefficient value for the reaction of myrcene with NO<sub>2</sub> measured in this work is in good agreement with those obtained by Orlando et al.,<sup>10</sup> Reissell et al.,<sup>11</sup> and Atkinson et al.<sup>17</sup> Reissell et al.<sup>11</sup> indicated that in their work during the first 15–20 min of the reaction, the decay rate of myrcene was fast and decreased over the course of the reaction time. These authors suggested the OH radicals formation due to the presence of NO ( $\text{NO} + \text{HO}_2 \rightarrow \text{NO}_2 + \text{OH}$ ) either originally present in the gas mixture or introduced with NO<sub>2</sub> might contribute to additional myrcene consumption.

For ocimene, the rate coefficient obtained in this work is in good agreement with those obtained by Reissell et al.<sup>11</sup> and Atkinson et al.<sup>17</sup> as shown in Table 1. In addition, we have conducted one run to estimate the reactivity of ocimene isomers toward NO<sub>2</sub> and obtained  $k(\text{cis-ocimene}) = k(\text{trans-ocimene}) \approx 7 \times 10^{-19} \text{ cm}^3 \text{ molecule}^{-1} \text{ s}^{-1}$ .

Finally, the rate coefficient value for the reaction of NO<sub>2</sub> with 1,3-cyclohexadiene is also in good agreement with the previous measurements.<sup>4,5,8</sup>

Examination of the reactivity of NO<sub>2</sub> with the four studied unsaturated VOCs shows the trend:  $k(1,3\text{-cyclohexadiene}) > k(\text{ocimene}) > k(\text{myrcene}) > k(\text{isoprene})$ . The four species possess a group of conjugated double carbon bonds ( $-\text{C}=\text{C}-\text{C}=\text{C}-$ ), which are the key reactive sites. The different reactivities observed mainly depend on the molecular structure and sites of their substitution groups to the conjugated dienes, revealing that the reactivity increases with the substitution degree of  $-\text{C}=\text{C}-\text{C}=\text{C}-$  groups which has been observed in this study and elsewhere.<sup>5,6</sup> The main difference between these four conjugated dienes is the degree of substitution. The difference in the reactivity of NO<sub>2</sub> with ocimene and myrcene shows that the reaction occurs mainly on the conjugated double bonds and the isolated  $-\text{C}=\text{C}(\text{CH}_3)_2$  does not play an important role.

**4.2. Oxidation Products.** A set of three to five experiments have been performed for each reaction. Reactants were monitored using the same procedure as mentioned in the kinetic section (section 4.1).

FT-IR spectra from NO<sub>2</sub>-initiated reactions of myrcene and ocimene have been first subtracted from HNO<sub>3</sub> and HONO, showing the presence of acetone and formic acid among the oxidation products. Examples of IR spectra obtained are presented in the Supporting Information. Plots of acetone versus the consumption of myrcene and ocimene are displayed



in Figure 3a,b, respectively. Acetone, the major identified product from  $\text{NO}_2$  reactions with myrcene and ocimene,

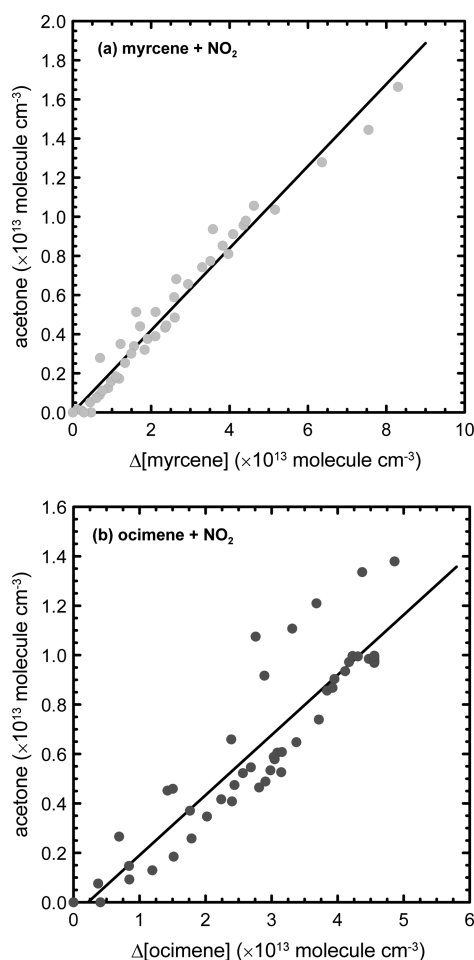


**Figure 3.** Acetone formation versus the consumed concentration of myrcene (a) and ocimene (b) during the reactions with  $\text{NO}_2$ .

accounted for  $22 \pm 3\%$  and  $26 \pm 7\%$ , respectively.  $\text{HCHO}$ ,  $\text{HCOOH}$ , and  $\text{CO}$  have been quantified at  $2.0 \pm 0.8\%$ ,  $0.7 \pm 0.2\%$ , and  $19 \pm 8\%$ , respectively, for the reaction of  $\text{NO}_2$  with myrcene and  $2.1 \pm 1.6\%$ ,  $1.1 \pm 0.5\%$ , and  $11 \pm 5\%$ , respectively, for the reaction of  $\text{NO}_2$  with ocimene.  $\text{HONO}$  formation yields have been estimated to  $3.5 \pm 1.3\%$  for myrcene and  $4.1 \pm 1.2\%$  for ocimene. Previous work conducted on the  $\text{NO}_2$  initiated oxidation of myrcene and ocimene reported only acetone as the reaction product. The formation yield of acetone from myrcene oxidation obtained in the present work is in disagreement with the reported ones in the literature estimated at  $11 \pm 3\%$ <sup>10</sup> and  $\sim 37\%$ .<sup>11</sup> The acetone formation yield for ocimene oxidation is in agreement with that reported by Reissell et al.<sup>11</sup> ( $\sim 28\%$ ). However, it has to be mentioned that the data of Reissell et al.<sup>11</sup> were derived from a single experiment and the use of a preconcentration system on adsorbent cartridge (Tenax) to collect gaseous compounds during analysis. Indeed, this method could lead to an overestimation of reaction products in the terpene- $\text{NO}_x$ -air system.<sup>18</sup> The difference observed with the reported value of Orlando et al.<sup>10</sup> remains unexplained so far. We have not observed the formation of nitrogen-containing compounds as products of the reactions  $\text{NO}_2$  + myrcene and  $\text{NO}_2$  + ocimene. This may indicate that these types of products are not formed

at all or formed at concentration levels below the detection limit of our analytical system.

FT-IR analyses of isoprene/ $\text{NO}_2$ /air and 1,3-cyclohexadiene/ $\text{NO}_2$ /air mixtures have shown the formation in time of nitro-organic compounds, as shown the IR spectra on Figure 4a,b. In the case of isoprene, we have observed an increase of IR

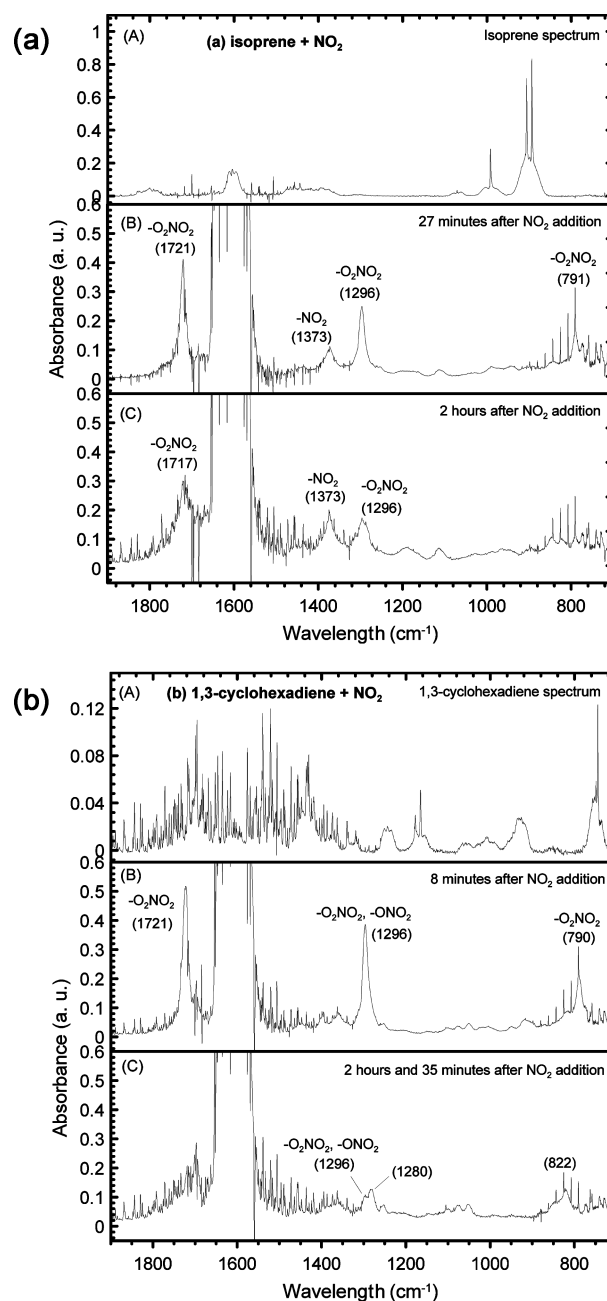


**Figure 4.** FT-IR spectra of products recorded in the range  $1900 - 700 \text{ cm}^{-1}$  from the  $\text{NO}_2$ -initiated reaction of isoprene (a) and 1,3-cyclohexadiene (b). Panels A are the recorded spectra of isoprene and 1,3-cyclohexadiene, before  $\text{NO}_2$  addition on the Figure 4a,b, respectively. Panels B have been recorded at 27 and 8 min after  $\text{NO}_2$  addition for isoprene and 1,3-cyclohexadiene, respectively. Panels C have been recorded 2 and 2 h and 35 min after  $\text{NO}_2$  addition for isoprene and 1,3-cyclohexadiene, respectively. Spectra in panels B and C have been subtracted from isoprene (Figure 4a) and 1,3-cyclohexadiene (Figure 4b) and known products (nitrous acid, nitric acid, and formic acid for isoprene/ $\text{NO}_2$  system).

absorption bands centered at 1721, 1296, and 791  $\text{cm}^{-1}$  assigned to  $-\text{OONO}_2$  and at 1373  $\text{cm}^{-1}$  assigned to  $-\text{NO}_2$  groups.<sup>19,20</sup> An example of the recorded spectra resulting from the  $\text{NO}_2$  reaction with isoprene in 760 Torr of air is shown in Figure 4a. IR band features of identified product species have been subtracted from these spectra. Major IR bands from spectra B and C have been assigned to nitrogen-containing compounds,  $-\text{O}_2\text{NO}_2$  and  $-\text{NO}_2$  groups. However, in the absence of FT-IR reference spectra, their quantifications were not possible. Figure 5 displays an example of the temporal

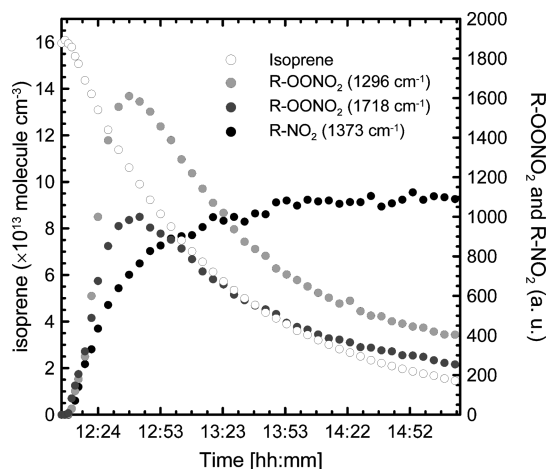


**Figure 5.** Time concentration profiles of  $\text{R-OONO}_2$  and  $\text{R-NO}_2$  type products from  $\text{NO}_2$ -initiated reaction of isoprene in the dark.

profiles of the IR bands intensities attributed to the  $-\text{OONO}_2$  and  $-\text{NO}_2$  groups, obtained from the subtraction of the residual spectra assigned as reference spectra, versus the consumed fraction of isoprene over the course of the experiment. Figure 5 shows a rapid formation at an earlier stage of the reaction and a decrease over the reaction time for the  $\text{R-OONO}_2$  compound while bands assigned to  $\text{R-NO}_2$  show a linear increase before reaching a plateau against the consumed fraction of isoprene. HONO has been also observed at low concentrations, and its formation has been estimated to be  $3.5 \pm 1.8\%$ . HCHO, HCOOH, and CO have been identified among the oxidation products but are mainly formed as secondary products. Their primary formation yields have been estimated to be  $1.3 \pm 0.6\%$ ,  $0.7 \pm 0.5\%$ , and  $0.9 \pm 0.3\%$  for HCHO, HCOOH, and CO, respectively. Analysis of  $\text{NO}_2$ -initiated oxidation of 1,3-cyclohexadiene data has shown intense peaks that can also be assigned to nitrogen-containing groups (Figure 4b). Panel B shows three strong bands located at 1721, 1296, and 790  $\text{cm}^{-1}$  characteristic of  $-\text{O}_2\text{NO}_2$  groups, which could be attributed to the formation of nitrocyclohexenylperoxy nitrate.<sup>8</sup> From panel C, it can be seen that these compounds exhibit a strong reaction time variability. For a longer reaction time, peaks assigned to  $-\text{O}_2\text{NO}_2$  groups decreased while the IR bands at 1280 and 822  $\text{cm}^{-1}$  increased. HONO was also identified from the reaction of  $\text{NO}_2$  with 1,3-cyclohexadiene with a yield  $2.4 \pm 0.6\%$ , in agreement with that reported by Jenkin et al.,<sup>8</sup> estimated to be around 2%. In addition, Jenkin et al.<sup>8</sup> have identified benzene among the oxidation products from the reaction of 1,3-cyclohexadiene with  $\text{NO}_2$  at  $0.41 \pm 0.02\%$ . HCHO, CO, and HCOOH have been identified among the oxidation products but are mainly

formed from secondary sources. Their primary formation yields have been estimated to be  $<1\%$ .

**4.3. Reaction Mechanism.** The suggested mechanistic schemes of the reaction of myrcene and ocimene with  $\text{NO}_2$  are displayed in Figures 6 and 7, respectively. The reaction proceeds by addition of  $\text{NO}_2$  on conjugated double bonds  $>\text{C}=\text{C}-\text{C}=\text{C}<$ . For both compounds, the carbon in the sixth position is supposed to be unfavored due to a steric hindrance and a low electron delocalization. The expected addition site for  $\text{NO}_2$  is that on carbons 5 and 8 for ocimene and on carbons 8 and 10 for myrcene, leading to the formation of the allylic  $\text{C}=\text{C}-\text{C}^\bullet$  radical. Although leading to a less stable radical ( $\text{C}=\text{C}-\text{C}^\bullet$ ) than the allylic radical, addition of  $\text{NO}_2$  at position 7 on ocimene is also considered as a pathway leading to the observed acetone production. This leads to the formation of nitroalkyl radicals ( $\text{R-NO}_2$ ) through reaction 1. These addition sites are expected to occur due to the high stability of the nitroalkyl radical formed. It either reacts directly with  $\text{O}_2$  to form a nitroperoxyalkyl radical ( $\text{ROONO}_2$ ) and further with RO via reaction 5 or undergoes electron delocalization, leading to two other nitroalkyl radical intermediates as suggested through the equilibrium pathways 2.1. To lead to acetone formation, we have proposed an intramolecular cyclization of these intermediates (reaction 2.2 for myrcene and reactions 1.1 and 2.2 for ocimene), which would react quickly to form a nitroalkoxyl radical ( $\text{RONO}_2$ ) through reaction 3 for myrcene and reaction 5 for ocimene. Acetone might be formed through the decomposition of the nitroalkoxyl radical (reaction 4 for myrcene and reaction 6 for ocimene). From the  $\text{NO}_2$  reaction with myrcene, the decomposition of the nitroalkoxyl radical originated from the direct addition of  $\text{O}_2$ , without any resonance may lead to the formation of a carbonyl compound and  $\text{OCH}_2\text{NO}_2$  radical for myrcene +  $\text{NO}_2$  reaction. This latter decomposes to form  $\text{NO}_2$  and formaldehyde. The low formation yield of formaldehyde ( $<1\%$ ) shows that this reaction occurs to a minor extent.

The reaction of  $\text{NO}_2$  with 1,3-cyclohexadiene proceeds via  $\text{NO}_2$  addition on the double bond, leading to the formation of a nitrohexenyl radicals.<sup>4,8</sup> The addition of  $\text{NO}_2$  on the terminal bond is favored due to the stability-resonance of the radical formed. An unpaired electron is removed by electronic delocalization. A rapid reaction with oxygen leads to the formation of a nitroperoxyhexenyl radical, which further reacts with  $\text{NO}_2$ .

The mechanism proposed for the reaction of isoprene with  $\text{NO}_2$  is based on the studies of the reaction of 1,3-butadiene ( $\text{CH}_2=\text{CHCH}=\text{CH}_2$ ) with  $\text{NO}_2$  proposed by Calvert et al.,<sup>2</sup> Atkinson et al.,<sup>5</sup> and Niki et al.,<sup>19</sup> which proceeds by electrophilic addition on the double bond  $>\text{C}=\text{C}<$ . A proposed scheme for the reaction of isoprene with  $\text{NO}_2$  is given in the Supporting Information. As shown in the FT-IR spectra (Figure 4a), formation of  $-\text{O}_2\text{NO}_2$  and  $-\text{ONO}_2$  compounds have been identified from the beginning of the reaction.  $\text{NO}_2$  will add predominantly to C1 due to the formation of the most substituted nitroalkyl radical.  $\text{NO}_2$  addition on C4 is expected to lead to the formation of a less stable secondary alkyl radical, which may, however, also occur to some extent. Additions to C2 and C3 appear to be unlikely due to a low stability of the radical formed. The nitroalkyl radical,  $\text{R-NO}_2$ , will form a nitroperoxy radical ( $\text{RNO}_2-\text{OO}^\bullet$ ), which in turn reacts with  $\text{NO}_2$ , leading to a dinitroperoxy nitrate ( $\text{RNO}_2-\text{OONO}_2$ ). The alkyl peroxyxynitrate may decompose back to the peroxy radical. The experiments





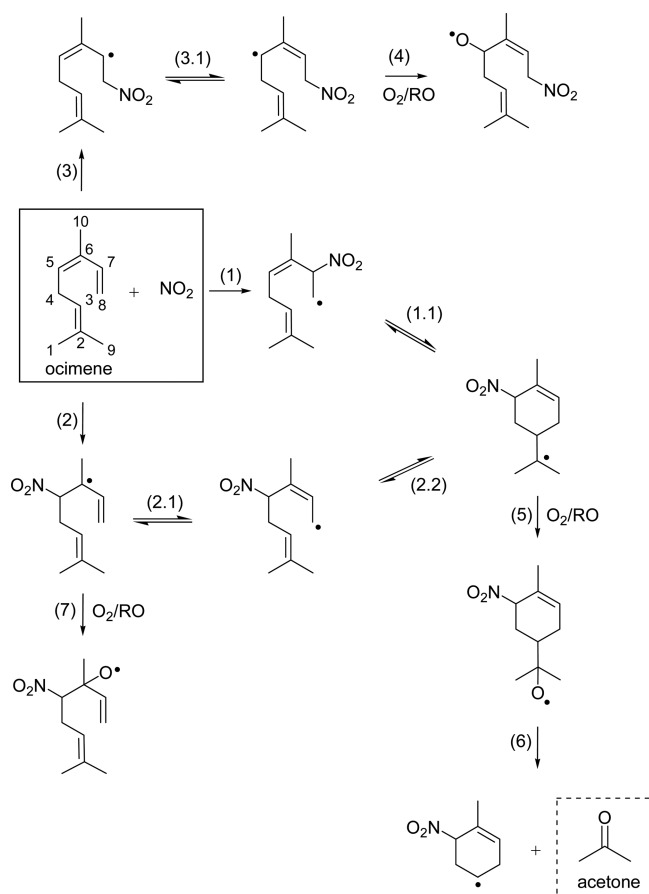


**Figure 7.** Proposed mechanism for the reaction of  $\text{NO}_2$  with ocimene in the dark.

those conditions, be of some, albeit minor, importance. This may also be the case at the edges of fossil-fueled power plant plumes in polluted urban air masses, where mixing of  $\text{NO}_2$ -rich power plant plumes interact with the VOCs of polluted air masses. The  $\text{NO}_2$  level is often found to be higher in indoor environments than in outdoor ones due to internal sources originating from combustion processes such as cooking, cigarettes, unvented heaters, leading to a  $\text{NO}_2$  concentration up to ppm level.<sup>29–31</sup> Besides, secondary  $\text{NO}_2$  can be produced from the dark conversion of  $\text{NO}$  by  $\text{O}_3$ . Therefore, the  $\text{NO}_2$  reaction is likely to occur in an indoor atmosphere with a higher level of alkenes. Hence, this process could constitute a non-negligible atmospheric source of the nitro-containing compounds in some specific areas. Indeed, the present work has shown that the reactions of  $\text{NO}_2$  with the investigated alkenes may lead to the formation of a series of nitrogen-containing oxygenated VOCs such as  $\text{RNO}_2$  and  $\text{ROONO}_2$ , though this assumption was not confirmed through the use of authentic samples. This observation is of importance because the nitro-containing compounds are known to be toxic to humans.<sup>32,33</sup> Hence, this process may contribute to the nitro-compounds budget even with a low reactivity. Furthermore, possible formation of nitrous acid from the reactions alkene +  $\text{NO}_2$  has been observed in this study with formation yields in the range 2.4–4.1% for the investigated alkenes, indicating that this process may not contribute significantly to the HONO budget. The reaction of other organic compounds, having a larger reactivity toward  $\text{NO}_2$ , such as  $\alpha$ -terpinene and  $\alpha$ -

phellandrene, may have higher contributions to both nitro-organic compounds and HONO.

## ■ ASSOCIATED CONTENT

### Supporting Information

Summary of the experimental conditions and the results of the absolute rate study from the reaction of  $\text{NO}_2$  with alkenes (isoprene, myrcene, ocimene, and 1,3-cyclohexadiene) is available. A graph obtained of the relative rate measurements from the  $\text{NO}_2$ -initiated reaction of ocimene using myrcene as reference organic compound in the presence of an excess of di-*n*-butylether can be also found. In addition, FT-IR spectra of products recorded in the range  $1900\text{--}700\text{ cm}^{-1}$  from the  $\text{NO}_2$ -initiated reaction of myrcene (a) and ocimene (b) are provided. A proposed mechanism of the  $\text{NO}_2$ -initiated reaction of isoprene in the dark is also included. Complete author lists for refs 7 and 28 are provided. This material is available free of charge via the Internet at <http://pubs.acs.org>.

## ■ AUTHOR INFORMATION

### Corresponding Author

\*A. Mellouki: tel, +33 (0) 2 38 25 76 12; fax, +33 (0) 2 38 69 60 04; e-mail, [mellouki@cnrs-orleans.fr](mailto:mellouki@cnrs-orleans.fr).

### Notes

The authors declare no competing financial interest.

## ■ ACKNOWLEDGMENTS

This work has been supported by the European FP7 EUROCHAMP 2 project, the IRSES-EU project “AMIS” and the Labex Voltaire (ANR-10-LABX-100-01).

## ■ REFERENCES

- (1) Atkinson, R.; Arey, J. Gas-Phase Tropospheric Chemistry of Biogenic Volatile Organic Compounds: A Review. *Atmos. Environ.* **2003**, *37*, S197–S219.
- (2) Calvert, J. G.; Atkinson, R.; Kerr, J. A.; Madronich, S.; Moortgat, G. K.; Wallington, T. J.; Yarwood, G. *The Mechanisms of Atmospheric Oxidation of the Alkenes*; Oxford University Press Inc: New York, 2000.
- (3) Stabel, J. R.; Johnson, M. S.; Langer, S. Rate Coefficients for the Gas-Phase Reaction of Isoprene with  $\text{NO}_3$  and  $\text{NO}_2$ . *Int. J. Chem. Kinet.* **2005**, *37*, 57–65.
- (4) Ohta, T.; Nagura, H.; Suzuki, S. Rate Constants for the Reactions of Conjugated Olefins with  $\text{NO}_2$  in the Gas Phase. *Int. J. Chem. Kinet.* **1986**, *18*, 1–11.
- (5) Atkinson, R.; Aschmann, S. M.; Winer, A. M.; Pitts, J. N. J. Gas Phase Reaction of  $\text{NO}_2$  with Alkenes and Dialkenes. *Int. J. Chem. Kinet.* **1984**, *16*, 697–706.
- (6) Glasson, W. A.; Tuesday, C. S. The Atmospheric Thermal Oxidation of Nitric Oxide in the Presence of Dienes. *Environ. Sci. Technol.* **1970**, *4*, 752–757.
- (7) Guenther, A.; Hewitt, N. C.; Erickson, D.; Fall, R.; Geron, C.; Graedel, T.; Harley, P.; Klinger, L.; Lerdau, M.; McKay, W. A.; et al. A Global Model of Natural Volatile Organic Compound Emissions. *J. Geophys. Res.* **1995**, *100*, 8873–8892.
- (8) Jenkin, M. E.; Sulbaek Andersen, M. P.; Hurley, M. D.; Wallington, T. J.; Taketani, F.; Matsumi, Y. A Kinetics and Mechanistic Study of the OH and  $\text{NO}_2$  Initiated Oxidation of Cyclohexa-1,3-diene in the Gas Phase. *Phys. Chem. Chem. Phys.* **2005**, *7*, 1194–1204.
- (9) Reissell, A.; Aschmann, S. M.; Atkinson, R.; Arey, J. Products of the OH Radical- and  $\text{O}_3$ -Initiated Reactions of Myrcene and Ocimene. *J. Geophys. Res.* **2002**, *107*, ACH 3–1–ACH3–6.
- (10) Orlando, J. J.; Nozière, B.; Tyndall, G. S.; Orzechowska, G. E.; Paulson, S. E.; Rudich, Y. Product Studies of the OH- and Ozone-Initiated Oxidation of some Monoterpenes. *J. Geophys. Res.* **2000**, *105*, 11561–11572.

- (11) Reissell, A.; Harry, C.; Aschmann, S. M.; Atkinson, R.; Arey, J. Formation of Acetone from the OH Radical- and O<sub>3</sub>-Initiated Reactions of a Series of Monoterpenes. *J. Geophys. Res.* **1999**, *104*, 13869–13879.
- (12) Bernard, F.; Daële, V.; Mellouki, A.; Sidebottom, H. Studies of the Gas Phase Reactions of Linalool, 6-Methyl-5-hepten-2-ol and 3-Methyl-1-penten-3-ol with O<sub>3</sub> and OH Radicals. *J. Phys. Chem. A* **2012**, *116*, 6113–6126.
- (13) Bernard, F.; Eyglunet, G.; Daële, V.; Mellouki, A. Kinetics and Products of Gas-Phase Reactions of Ozone with Methyl Methacrylate, Methyl Acrylate, and Ethyl Acrylate. *J. Phys. Chem. A* **2010**, *114*, 8376–8383.
- (14) Calvert, J. G.; Mellouki, A.; Orlando, J. J.; Pilling, M. J.; Wallington, T. J. *The Mechanisms of Atmospheric Oxidation of the Oxygenates*; Oxford University Press Inc: New York, 2011.
- (15) Paulson, S. E.; Flagan, R. C.; Seinfeld, J. H. Atmospheric Photooxidation of Isoprene - Part I: The Hydroxyl Radical and Ground State Atomic Oxygen Reactions. *Int. J. Chem. Kinet.* **1992**, *24*, 79–101.
- (16) Gu, C.-I.; Rynard, C. M.; Hendry, D. G.; Mill, T. Hydroxyl Radical Oxidation of Isoprene. *Environ. Sci. Technol.* **1985**, *19*, 151–155.
- (17) Atkinson, R.; Aschmann, S. M.; Winer, A. M.; Pitts, J. N. J. Kinetics and Atmospheric Implications of the Gas-Phase Reactions of NO<sub>3</sub> Radicals with a Series of Monoterpenes and Related Organics at 294 ± 2 K. *Environ. Sci. Technol.* **1985**, *19*, 159–163.
- (18) Pommer, L.; Fick, J.; Andersson, B.; Nilsson, C. Development of a NO<sub>2</sub> Scrubber for Accurate Sampling of Ambient Levels of Terpenes. *Atmos. Environ.* **2002**, *36*, 1443–1452.
- (19) Niki, H.; Maker, P. D.; Savage, C. M.; Breitenbach, L. P.; Hurley, M. D. An FTIR Spectroscopic Study of the Kinetics and Mechanism for the NO<sub>2</sub>-Initiated Oxidation of Tetramethyl Ethylene at 298 K. *Int. J. Chem. Kinet.* **1986**, *18*, 1235–1247.
- (20) Tuazon, E. C.; Atkinson, R. A Product Study of the Gas-Phase Reaction of Isoprene with the OH Radical in the Presence of NO<sub>x</sub>. *Int. J. Chem. Kinet.* **1990**, *22*, 1221–1236.
- (21) Tyndall, G. S.; Cox, R. A.; Granier, C.; Lesclaux, R.; Moortgat, G. K.; Pilling, M. J.; Ravishankara, A. R.; Wallington, T. J. Atmospheric Chemistry of Small Organic Peroxy Radicals. *J. Geophys. Res.* **2001**, *106*, 12157–12182.
- (22) Hornbrook, R. S.; Crawford, J. H.; Edwards, G. D.; Goyea, O.; Mauldin, R. L., III; Olson, J. S.; Cantrell, C. A. Measurements of Tropospheric HO<sub>2</sub> and RO<sub>2</sub> by Oxygen Dilution Modulation and Chemical Ionization Mass Spectrometry. *Atmos. Meas. Tech.* **2011**, *4*, 735–756.
- (23) Witter, M.; Berndt, T.; Böge, O.; Stratmann, F.; Heintzenberg, J. Gas-Phase Ozonolysis: Rate Coefficients for a Series of Terpenes and Rate Coefficients and OH Yields for 2-Methyl-2-butene and 2,3-Dimethyl-2-butene. *Int. J. Chem. Kinet.* **2002**, *34*, 394–403.
- (24) Atkinson, R.; Aschmann, S. M.; Pitts, J. N. J. Rate Constants for the Gas-Phase Reactions of the OH Radical with a Series of Monoterpenes at 294 ± 1 K. *Int. J. Chem. Kinet.* **1986**, *18*, 287–299.
- (25) Ghude, S. D.; Fadnavis, S.; Beig, G.; Polade, S. D.; Van der A, R. J. Detection of Surface Emission Hot Spots, Trends, and Seasonal Cycle from Satellite-Retrieved NO<sub>2</sub> over India. *J. Geophys. Res.* **2008**, *113*, D20305.
- (26) Sheel, V.; Lal, S.; Richter, A.; Burrows, J. P. Comparison of Satellite Observed Tropospheric NO<sub>2</sub> over India with Model Simulations. *Atmos. Environ.* **2010**, *44*, 3314–3321.
- (27) Richter, A.; Burrows, J. P.; Nü, H.; Granier, C.; Niemeier, U. Increase in Tropospheric Nitrogen Dioxide over China Observed from Space. *Nature* **2005**, *437*, 129–132.
- (28) Lou, S.; Holland, F.; Rohrer, F.; Lu, K.; Bohn, B.; Brauers, T.; Chang, C. C.; Fuchs, H.; Häseler, R.; Kita, K.; et al. Atmospheric OH Reactivities in the Pearl River Delta – China in Summer 2006: Measurement and Model Results. *Atmos. Chem. Phys.* **2010**, *10*, 11243–11260.
- (29) WHO Guidelines for Indoor Air Quality: Selected Pollutants; WHO Regional Office for Europe, 2010; <http://www.euro.who.int/> data/assets/pdf\_file/0009/128169/e94535.pdf (accessed Jul 31, 2013).
- (30) *Indoor Pollution by NO<sub>2</sub> in European Countries*; Commission of the European Communities, Directorate General for Science, Research and Development, Joint Research Centre - Institute for the Environment, COST project 613 - Report No. 3, Ispra Establishment. EUR 12219 EN, 1989; [http://www.inive.org/medias/ECA/ECA\\_Report3.pdf](http://www.inive.org/medias/ECA/ECA_Report3.pdf) (accessed Jul 31, 2013).
- (31) United States Environmental Protection Agency Website; <http://www.epa.gov/iaq/no2.html> (accessed Jul 31, 2013).
- (32) Purohit, V.; Basu, A. K. Mutagenicity of Nitroaromatic Compounds. *Chem. Res. Toxicol.* **2000**, *13*, 673–692.
- (33) Kawai, A.; Goto, S.; Matsumoto, Y.; Matsushita, H. Mutagenicity of Aliphatic and Aromatic Nitro compounds. Industrial Materials and Related Compounds. *Jpn. J. Ind. Health* **1987**, *29*, 34–54.